applied sciences

MDPI

Article

Study on Compaction Characteristics and Compaction Process of an Unsaturated Silt Based on PFC3D

Zhitao Ma, Keyu Lu *, Daifu Song, Wenhu Liu, Yipeng Wang and Shunhai Li

College of Energy and Mining Engineering, Shandong University of Science and Technology, Qingdao 266590, China
* Correspondence: llkkyy555@163.com

Abstract: In order to reduce the construction cost of excessively wet silt roadbeds and improve the compaction quality, this paper studies the compaction characteristics and compaction technology of excessively wet silts through theoretical derivation, indoor experiments, numerical simulation, engineering verification, and other research methods. Based on the pendulum-type liquid bridge structure, this paper uses the Hertz–Mindlin theory, particle motion equation of state, and other theories to modify the force between particles of an unsaturated soil. Through the contact angle, which is a medium, the matrix suction is linked to the water content and is used to approximate the water content state of soil samples. Using PFC3D (particle flow code 3D) numerical simulation software, an unsaturated silt model was established based on Hill contact, and the model parameters were calibrated through basic geotechnical tests and triaxial compression tests. The correctness of the theory is verified by comparing the simulated triaxial compression test of wet silts with the indoor test. By simulating subgrade rolling, considering factors such as the distribution of contact force chain and the variation of compaction degree, the effects of rolling times, strong vibration, and weak vibration on the compaction effect were compared and analyzed. Finally, the optimal rolling and compaction process under the optimal water content is obtained through on-site engineering tests. The results show that: (1) The Hill contact model is reasonable for simulating the wet silt. (2) During the simulation of the roadbed compaction process using PFC3D software, it was found that the compaction degree change during the entire compaction process can be roughly divided into the initial compaction stage and the re-compaction stage. The reasonable number of compaction times was determined to be five through discrete element simulation. (3) It is found from the numerical simulation results that compared to static compaction, both strong and weak vibration compaction can effectively improve the compaction effect of subgrade compaction. The larger the vibration amplitude, the more obvious the improvement of the compaction effect. The compaction effect of strong vibration followed by weak vibration is stronger than that of weak vibration followed by strong vibration. (4) The optimal compaction process obtained under the optimal moisture content of 15% is static pressure once + strong vibration twice + weak vibration twice.

Keywords: unsaturated silt; discrete element; hill contact; compaction characteristics; compaction process

check for updates

Citation: Ma, Z.; Lu, K.; Song, D.; Liu, W.; Wang, Y.; Li, S. Study on Compaction Characteristics and Compaction Process of an Unsaturated Silt Based on PFC3D. *Appl. Sci.* **2023**, *13*, 5547. https://doi.org/10.3390/app13095547

Academic Editors: Mien Jao and Mian C. Wang

Received: 28 March 2023
Revised: 27 April 2023
Accepted: 28 April 2023
Published: 29 April 2023

1. Introduction

An unsaturated silt is a kind of cohesive soil with a strong hydrophilicity and water holding capacity, and poor water permeability. It is distributed within layers on the surface. Its soil has special properties, large porosity, and viscosity, and generally contains expansive minerals, which makes it difficult to dry and not easy to crush [1]. At present, domestic and foreign scholars have carried out in-depth and systematic research on the physical and mechanical properties and compaction characteristics of unsaturated soils mainly through laboratory tests and numerical simulations [2–5].

For the mechanical properties of unsaturated soil, Guo et al. [6] simulated the deformation mechanism and mechanical properties of coarse-grained soil at the mesoscopic level.

Uniaxial compression tests were carried out on samples of different sizes to determine the distribution of particle strength and elastic modulus of the sample. The strength and elastic modulus of the sample particles decreases with the increase in particle size. Based on the idea of the discrete element method and the principle of pore elasticity, Kuhn et al. [7,8] analyzed the stress of soil samples under different particle combinations and calculated the pore fluid pressure of unsaturated soil. Liu et al. [9] simulated the water-bearing characteristics of unsaturated soils by adding adhesion force at the contact of particles, and compared the discrete element simulation results with the laboratory test results to verify the rationality and accuracy of the application of the adhesion force. Liu [10] used the discrete element numerical analysis software, MatDEM (matrix discrete element) and PFC (particle flow code), to study and analyze the unsaturated soil by the control variable method. The relationship between the macroscopic parameters of the unsaturated soil and the microscopic parameters of the discrete element model were calibrated, and the accuracy of the lsy liquid bridge contact model to simulate the unsaturated soil was verified. Zhou et al. [11] used Hill contact to consider the contact between soil particles, and established a discrete element model of unsaturated soil static triaxial test. The water content state of unsaturated soil was characterized by suction, and the influence of water content change on the stress–strain curve of the sample was obtained. In terms of rolling compaction characteristics, based on the discrete element method, Zhang et al. [12] improved the rolling compaction simulation from four aspects: micro-particle generation, boundary condition setting, real-time monitoring, and macro-meso parameter correspondence. The rolling compaction model was established more realistically and efficiently, and the effects of rolling combination mode, particle gradation, and particle appearance shape on compaction degree were discussed. Yan et al. [13] tested the soil in the Huaning section, improved the compaction degree of the silt roadbed, and reduced the cost of the roadbed construction by changing the construction technology of the silt roadbed. Cai et al. [14] solved the problem of rolling compaction of water-shortage or unsaturated silt road by using the variable amplitude rolling technology of static pressure-strong vibration-weak vibration-static pressure.

The international research on unsaturated soil mainly focuses on the characterization of water content, especially the influence of microscopic parameters on water content, while there is less research on rolling compaction technology. Therefore, the main purpose of this article is to (1) analyze the contact effect between unsaturated silt particles through theoretical derivation. Using the Hertz–Mindlin theory [15], particle motion equation of state, and other theories to modify the interaction forces between unsaturated soil particles, and by using the contact angle as the intermediate, the matrix suction is linked to the water content, and the soil moisture state is approximately characterized by the matrix suction. (2) By combining indoor experiments with numerical simulations, the micro-parameters of numerical simulations were calibrated to verify the correctness of the Hill contact model in simulating an unsaturated soil. (3) By simulating different construction processes of unsaturated soil roadbeds and comparing the changes in compaction degree and contact force chain, the optimal construction process of unsaturated silt roadbeds is determined. (4) Finally, the best construction plan is applied to the construction site of the Jingtai Expressway. From the feedback of the on-site construction plan, it can be seen that the best construction process on site is consistent with the best construction process obtained through discrete element simulation.

2. Analysis of the Contact Effect between Particles of an Unsaturated Silt

The PFC3D software is a particle flow analysis program developed by ITASA Consulting Group in the United States. The software is a numerical computing platform based on mesoscopic discrete element theory. It has been widely used in simulated geotechnical engineering. The advantage of this software is that it can automatically simulate the change characteristics of the soil basic properties in a stress environment. The mechanical properties of engineering an unsaturated silty soil can be well simulated by setting the mesoscopic parameters of the model through the combination of laboratory tests and simulated laboratory tests. The discrete element method allows for finite displacement of particles and a complete separation of rotating particles, and can automatically identify new contacts in the calculation process, which can make the simulation results more accurate. Therefore, this software is selected as a numerical simulation tool.

In the PFC3D version 5.0 software, spherical particles are the main skeleton structure that constitutes the discrete element model. The mechanical properties of the materials can be expressed by the contact between the particles. Different materials give different contact characteristics. The contact model in the PFC3D discrete element simulation software cannot characterize the mechanical properties of an unsaturated silt, a soil with water between pores, well. Based on the liquid bridge structure theory, Potyondy [16,17] improved the linear contact model in PFC3D, and obtained the Hill contact model that can reflect the characteristics of an unsaturated soil, as shown in Figure 1.

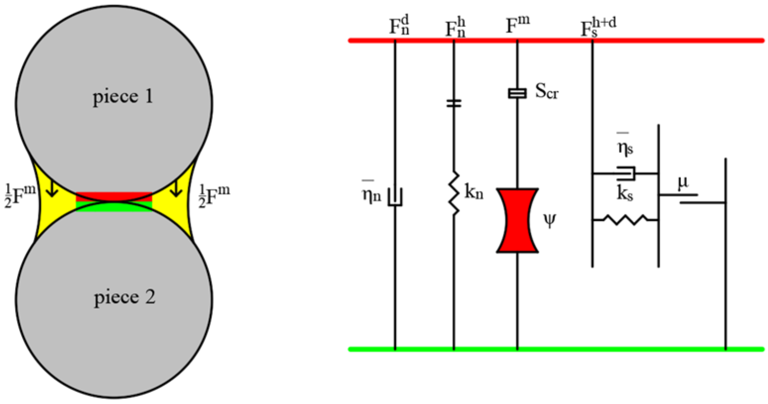

Figure 1. Hill contact diagram.

Compared with linear contact, Hill contact adds a suction force in the normal direction between particles to represent the water content of an unsaturated soil. The force-displacement law of the Hill contact can be expressed by Formula (1):

$$F^{\mathrm{c}} = F^{\mathrm{s}} + F^{\mathrm{m}}, M_{\mathrm{c}} = 0 \tag{1}$$

In the formula, F^{s} is the surface tension and F^{m} is the suction provided by the pore water.

When there is a liquid bridge structure between the particles, there will be the suction effect of pore water. When two particles contact directly, the suction effect is the largest. With the increase in particle spacing, the suction effect attenuates exponentially, until the critical spacing is reached. The relationship between the suction effect and particle spacing can be expressed by Formula (2):

$$F^m = \begin{cases} F^m_{\max}, g_c < 0 \\ F^m_{\max} \exp\left(\frac{-g_c}{2S_{cr}}\right), 0 \le g_c \le 2S_{cr} \\ 0, g_c > 2S_{cr} \end{cases} \tag{2}$$

In the formula, g_{c} is the particle spacing, $2S_{\mathrm{cr}}$ is the limit distance of the liquid bridge, S_{cr} is the radius of the smallest particle in the two particles, and S_{cr} = min(R1, R2), $F^m_{\max}$ is the maximum pore water pressure, which can be expressed by Formula (3).

$$F^m_{\max} = \psi(\pi S^2_{cr}) \tag{3}$$

In the formula, ψ is the matrix suction coefficient, which is related to the content of pore water between the particles.

3. Discrete Element Simulation of an Unsaturated Silt Static Triaxial Test

3.1. Modeling

The discrete element simulation process can be roughly divided into three stages: boundary constraint establishment, particle generation, and preloading. Firstly, according to the conventional indoor static triaxial test, the model rigid boundary constraint wall is generated according to the ratio of 1:1, and the wall size is a cylinder of φ39.1 mm * × 80 mm. Then the contact between the particles is set to Hill contact, and the particles are generated inside the wall according to the particle gradation.

The original particle size distribution curve obtained through particle analysis experiments is shown in Figure 2a. From the figure, it can be seen that the content of fine sand (0.002~0.075 mm) in the roadbed is relatively large, accounting for about 60%, while the proportion of the silt and clay (<0.002 mm) is relatively small, accounting for about 7%. In the process of constructing a discrete element model, a small particle size can lead to an increase in the number of generated particles, making calculation difficult. In order to simplify the calculation, particles smaller than 0.002 mm were filtered out during the generative model. In the PFC3D software, particles are generated by dividing the particle size intervals. In order to facilitate the construction of the model, each interval is grouped based on the slope of the straight line. Intervals with similar slopes are divided into one group, and the eight sections in the original grading curve are simplified into four sections (2~0.25 mm, 0.25~0.1 mm, 0.1~0.05 mm, 0.05~0.002 mm). The simplified grading distribution is shown in Figure 2b, and a static triaxial test discrete element model is constructed based on this particle grading curve.

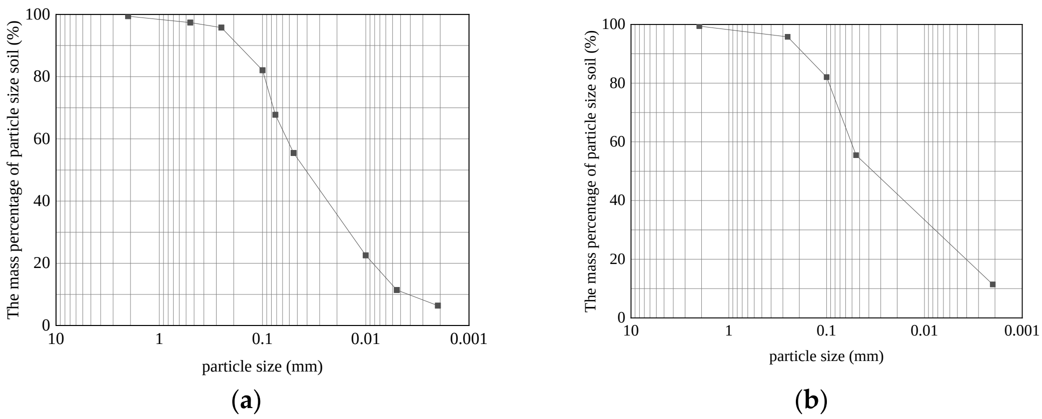

Figure 2. Particle grading curve. (**a**) Original gradation. (**b**) Simplified gradation.

In the process of indoor testing, the test soil sample is wrapped by a rubber membrane. Under the combined action of an axial load and circumferential confining pressure, due to the positive Poisson effect, the sample will produce an irregular lateral expansion. For the conventional discrete element model, the boundary constraint is a rigid wall, which is quite different from the indoor test and will have a certain impact on the simulation results. Therefore, the boundary conditions need to be adjusted to meet the flexible membrane boundary conditions. When establishing the flexible servo boundary, it is first necessary to delete the rigid boundary constraint. Then, at the rigid boundary position, the particles of the same particle size are used as the basic unit to generate the particle wall boundary. Then, the circumferential confining pressure is equivalent to the concentrated load, which is uniformly applied to each boundary particle. The contact between the boundary particles is set to linear contact, and finally, the flexible particle servo boundary is generated, as shown in Figure 3b.

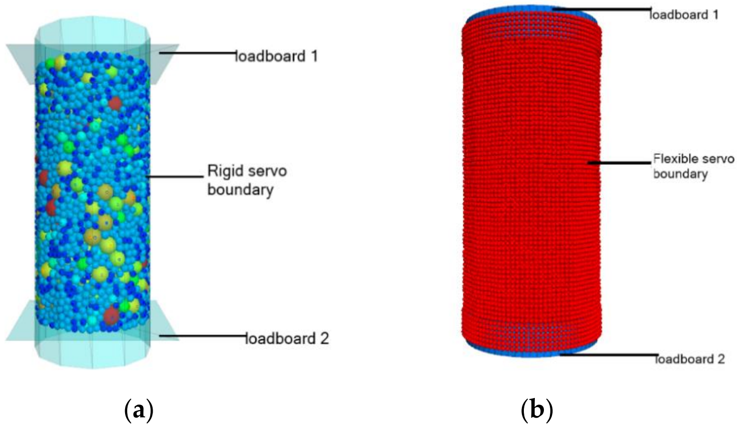

Figure 3. Discrete element model of the static triaxial test. (**a**) Rigid servo boundary. (**b**) Flexible servo boundary.

3.2. Calibration of Microscopic Parameters

In the process of discrete element simulation, the necessary test parameters are usually obtained through laboratory tests to provide a data basis for discrete element simulation. The test soil sample selected in this paper is an unsaturated silt in Pingyuan County, Dezhou Qihe River Section of the Beijing-Taizhou Expressway. Firstly, the basic physical properties of the soil sample are obtained through the basic geotechnical test, as shown in Table 1. Then, the unconsolidated undrained shear test is carried out on the TSZ-6A strain-controlled triaxial apparatus to obtain the stress–strain relationship curve of the sample under different confining pressure conditions, as shown in Figure 4. The water contents of the soil samples prepared by the triaxial test are 15%, 18%, and 21%, respectively, and the circumferential confining pressures are 100 KPa, 200 KPa, and 300 KPa, respectively.

Table 1. Basic physical properties of the soil samples.

Particle Diameter/mm	Relative Density of Particles	Liquid Limit/%	Plastic Limit/%	Plasticity Index/I_p	Soil Properties
0.002–2	2.70	32.3	23.6	8.7	low liquid limit silt

Based on laboratory test data, domestic and foreign scholars based the idea of inversion simulation [18] by changing the microscopic parameters of the model for a large number of static triaxial test discrete element simulations, the simulation results and laboratory test result comparative analysis through a trial and error method, to gradually determine the more reasonable discrete element model microscopic parameters. Figure 5a–d are the influence diagrams of the micro-parameters on the stress–strain curve when only the micro parameters, such as matrix suction, contact stiffness, friction coefficient, and damping coefficient, are changed. The indoor test data are the stress–strain curve obtained when the moisture content is 15% and the circumferential confining pressure is 200 kPa.

The key to the success of the simulation is to determine the meso parameters of the discrete element model efficiently and accurately. It can be seen from Figure 5 that the matrix suction mainly affects the peak stress of the curve, which is consistent with the influence trend of the water content on the test results. The contact stiffness mainly affects the slope of the curve, which is related to the contact effect between the particles. The change in the friction coefficient has a certain influence on the peak stress, and its effect is smaller than that of the matrix suction. The change in the damping coefficient has little effect on the simulation results.

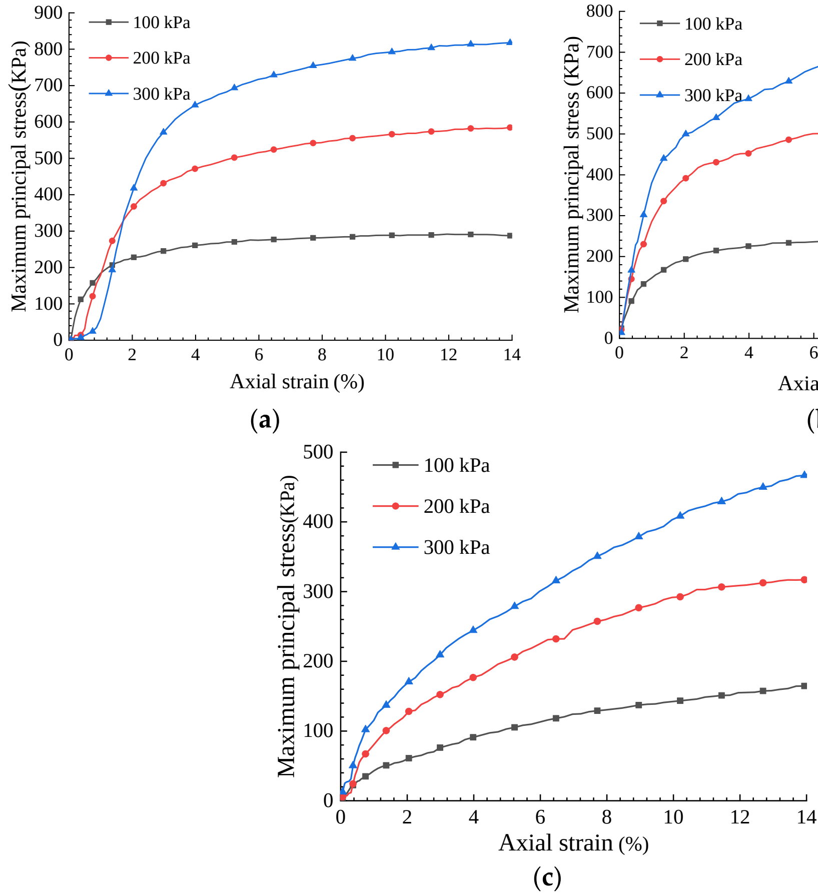

Figure 4. Stress–strain relationship curves of samples under different confining pressures. (**a**) Water content at 15%. (**b**) Water content at 18%. (**c**) Water content at 21%.

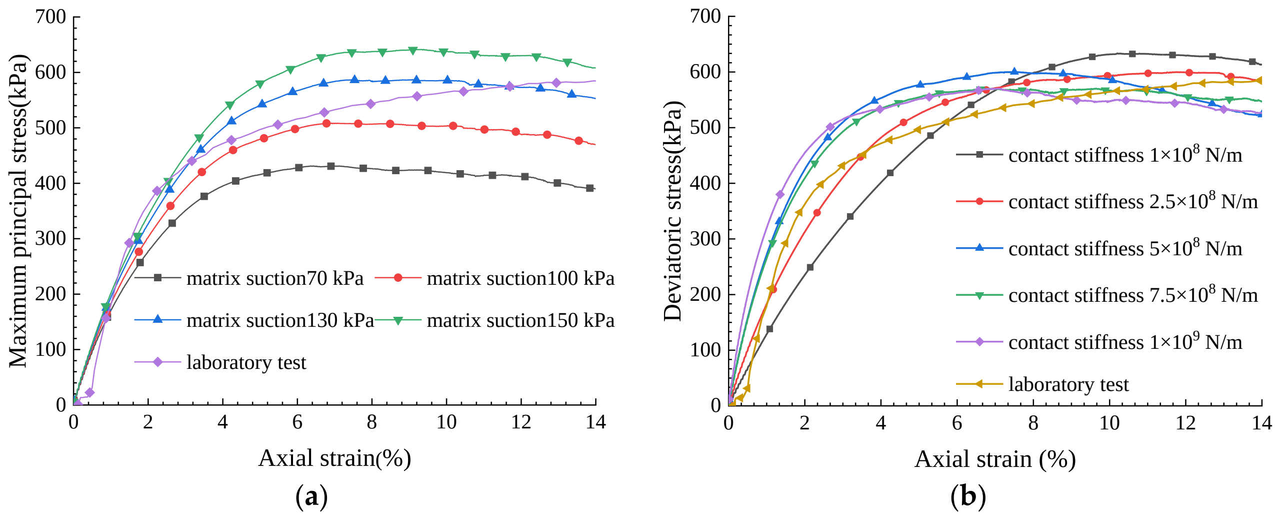

Figure 5. *Cont.*

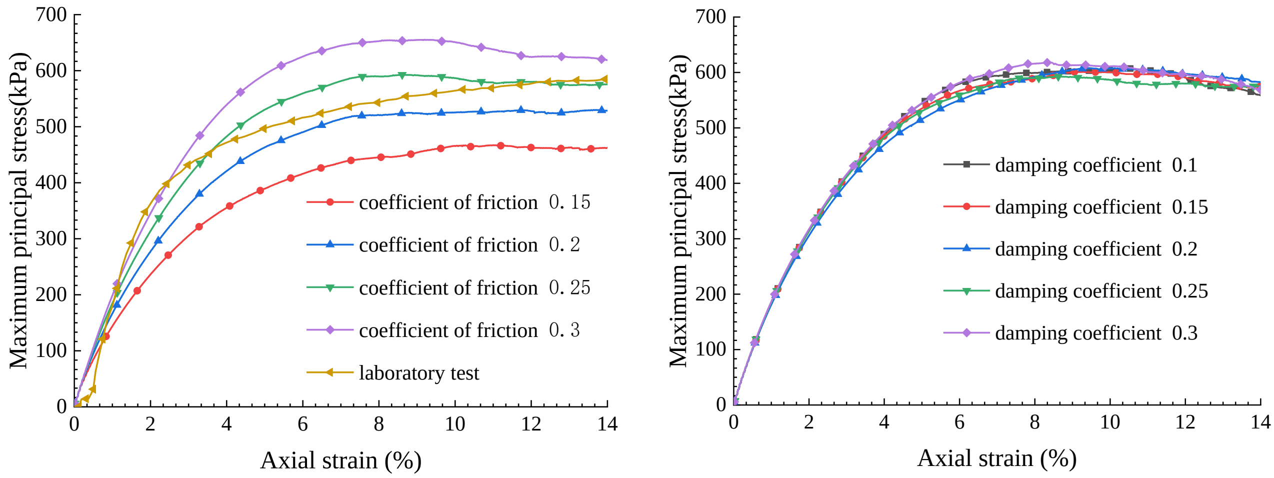

(**c**) (**d**)

Figure 5. Effect of meso-parameter changes on the stress–strain curve. (**a**) Matrix suction. (**b**) Contact stiffness. (**c**) Coefficient of friction. (**d**) Damping coefficient.

According to the influence of the microscopic parameters on the simulation results in Figure 5, a more reasonable microscopic parameter calibration step can be determined. The first parameter to be determined is the matrix suction, followed by the contact stiffness, and finally the damping coefficient and friction coefficient. Table 2 shows the calibrated Hill contact mesoscopic parameters concerning the indoor test results at 15% moisture content.

Table 2. Hill contact microscopic parameters.

Contact Stiffness/Pa	Suction/KPa	Damping Coefficient	Friction Coefficient
2.5×10^8	130	0.25	0.25

3.3. Rationality Verification of Discrete Element Simulation

Based on the microscopic parameters of the Hill contact in Table 2, the discrete element model of the static triaxial test is established. By changing the circumferential confining pressure, the discrete element simulation results are compared with the indoor test results to verify the rationality of using Hill contact to simulate an unsaturated silt. Figure 6 is the comparison of the stress–strain curves between discrete element simulation and laboratory test results under different confining pressure conditions, and Figure 7 is the comparison of the failure modes of samples.

From Figure 6, it can be seen that at the initial stage of loading, there is a certain gap between the indoor test and the discrete element simulation stress–strain curve, but the overall trend is consistent, the similarity between the two is high, and the peak stress that the two can reach is maintained at the same level. Therefore, it can be considered that it is reasonable and feasible to simulate the unsaturated silt with the Hill contact model. It can be seen from Figure 7 that under the action of an axial load, the failure modes of the two are also similar, showing the form of bulging failure, which also confirms the accuracy of using the Hill contact model to simulate an unsaturated soil.

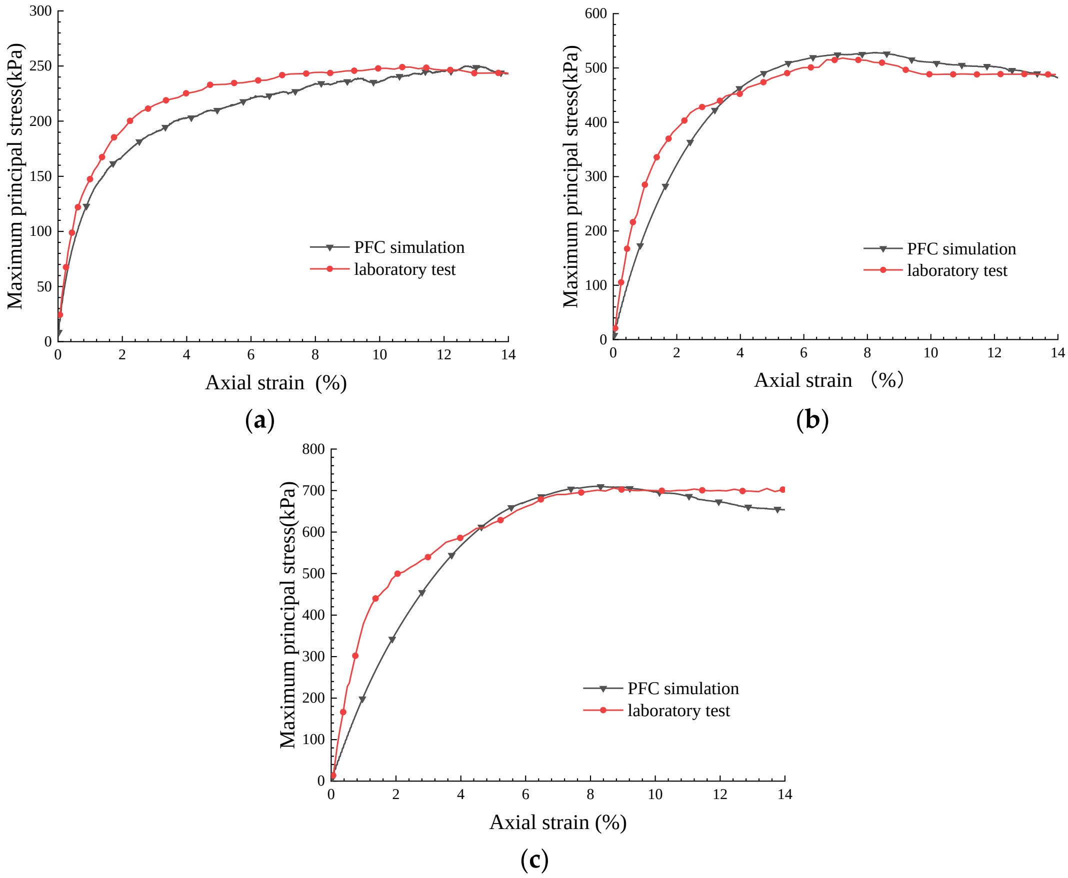

Figure 6. Comparison of discrete element simulation and laboratory test results. (**a**) Confining pressure 100 Kpa. (**b**) Confining pressure 200 Kpa. (**c**) Confining pressure 300 KPa.

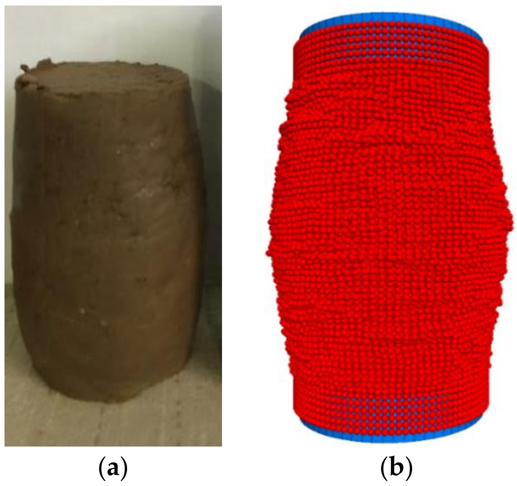

Figure 7. Comparison of failure modes between a laboratory test and a numerical simulation. (**a**) Laboratory test results. (**b**) Numerical simulation results.

4. Research on the Rolling Compaction Process

4.1. Modeling

In the construction of an unsaturated soil roadbed, the maximum dry density is usually selected as the standard dry density in the construction process, and the corresponding water content is the optimal water content of the rolling compaction. For the unsaturated silt in the section of the Jingtai Expressway, two sampling sites with far intervals were selected for sampling, respectively, and an indoor standard compaction test was carried out to obtain the relationship curve between dry density and water content, as shown in Figure 8. It can be seen from the figure that the optimal water content of the two sampling points is 15%. Therefore, in the discrete element simulation, the soil sample with 15% water content was selected for research.

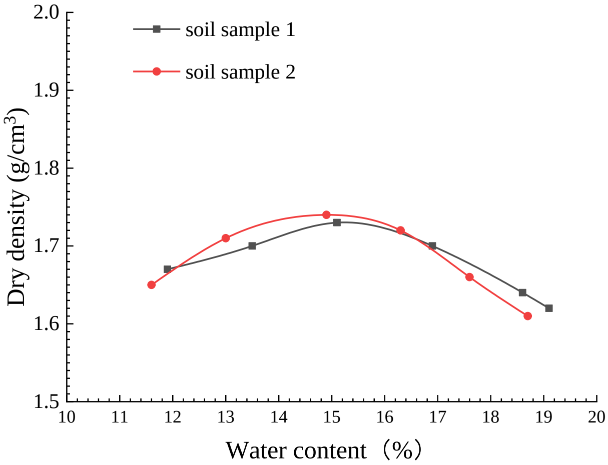

Figure 8. Indoor compaction test curve.

In this paper, a part of the unsaturated silt subgrade is selected as the research object, and a rolling model is established. The model size is 1 m × 0.29 m × 0.45 m. The contact between particles is set as the Hill contact. The contact parameters are taken from the Hill contact model parameters calibrated in Table 2. The particle size distribution is arranged according to the particle size distribution ratio in Figure 2b, and the particle size is scaled according to the overall size of the rolling compaction model.

When generating the particle element of the rolling model, to make the research results better, there are no sample preparation and preloading steps, but particles with a friction coefficient are directly generated, and then the particles are made to freely settle under the action of gravity. Finally, the model is leveled and the height of the leveled cutting surface is 0.09 m. Figure 9 is the rolling model after leveling.

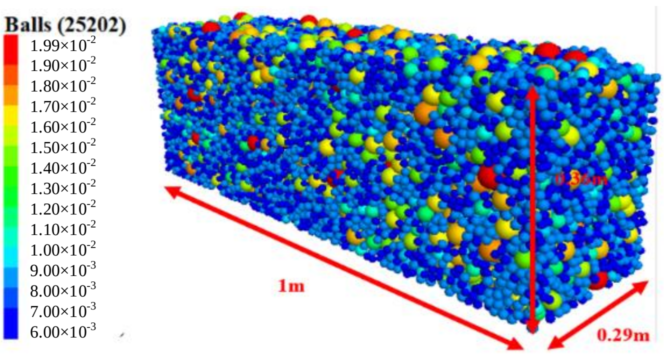

Figure 9. Rolling compaction model.

4.2. Loads Infliction

The rolling compaction model is established based on the similarity theory, and it also needs to be scaled when simulating the roller. The size of the scaled roller is 0.22 m in diameter and 0.29 m in height. Table 3 shows the motion parameters of the roller. In the PFC3D software, the wall element can be used to simulate the roller, but the wall element cannot directly apply the gravity load, so it is necessary to use servo control to equivalently replace the acting force of the roller on the soil. The servo force is calculated according to the weight of the roller and the excitation force generated by the eccentric rotation of the roller. The roller and compacted soil are in surface-to-surface contact, and there is only pressure interaction, but no tension. Therefore, the servo force, P, can be expressed by Formula (4):

$$P = \begin{cases} G + F_0 \sin(\omega t), & G + F_0 \sin(\omega t) \geq 0 \\ 0, & G + F_0 \sin(\omega t) < 0 \end{cases} \quad (4)$$

Table 3. Roller discrete element simulation parameter table.

Grinding Wheel Weight/N	Exciting Force/N	Vibration Frequency/Hz	The Gait of March/m*·s^{-1}
505	928	30	0.1

In the formula, P is the servo force of the compacted soil, G is the weight of the roller, and F_0 is the component force of the excitation force, F, in the vertical direction.

4.3. Analysis of the Compaction Results

4.3.1. Relationship between the Compaction Effect and Rolling Times

Figure 10 shows the relationship between the number of static rolling and the degree of compaction. It can be seen that the whole rolling process can be divided into two stages. The first stage is the initial rolling stage. Under the rolling action of the roller, the friction force and the liquid bridge force are overcome between the particles, the large and small particles are filled with each other, the porosity decreases rapidly, and the compaction degree of the model is improved obviously, such as during the first and second rolling. The second stage is the re-grinding stage. When the rolling model is compacted to a certain extent, the porosity is small, the particles are relatively stable, and it is not easy to move and fill. Under the rolling effect of the roller, the compaction degree of the sample is further reduced, but the compaction degree does not change significantly.

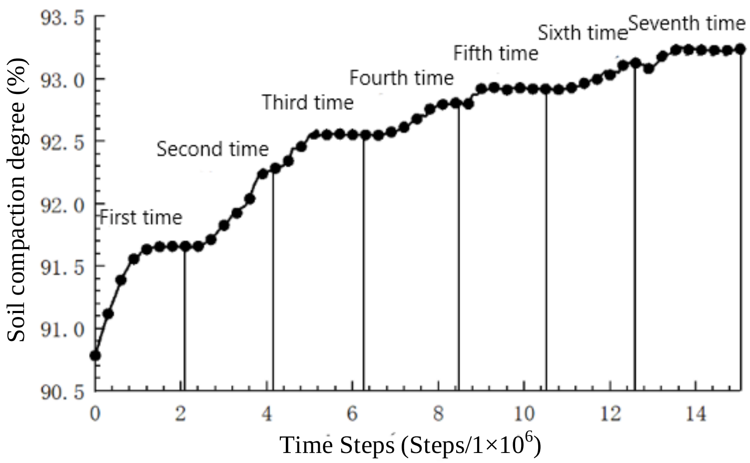

Figure 10. Relationship curve between the compaction degree and rolling times.

When analyzing the contact force chain between particles, it is necessary to set up a shear plane to analyze the contact force chain inside the model. Figure 11a–e shows the distribution of the particle contact force chain under different rolling times. Table 4 shows the numerical change in the contact force chain between the particles.

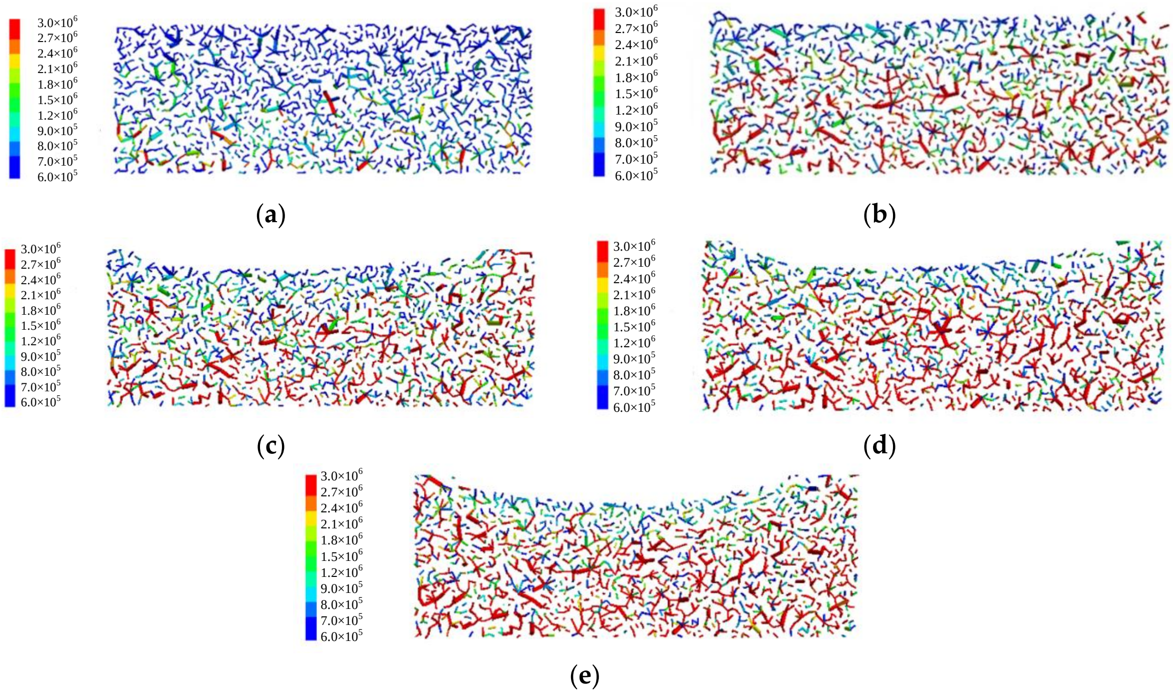

Figure 11. Distribution diagram of the contact force chain under different rolling times. (**a**) Not rolled. (**b**) Rolled once. (**c**) Rolled three times. (**d**) Rolled five times. (**e**) Rolled seven times.

Table 4. Table of the contact force chain changes under different rolling times.

Rolling Times	Contact Force Chain Size/N
0	2.52×10^5
1	6.84×10^5
2	1.06×10^6
3	1.35×10^6
4	1.74×10^6
5	1.98×10^6
6	2.14×10^6
7	2.23×10^6

From Figure 11 and Table 4, it can be seen that before the rolling operation, the distribution of the contact force chain between the particles is relatively uniform, and the value of the contact force chain is maintained at 2.52×10^5 N. With the continuous rolling, the contact force chain between the particles gradually tends to be dense, from the blue with a lower value, to the red with a higher value, and the closer to the bottom of the model, the denser the contact force chain is. After the second rolling, the growth amplitude of the contact force chain gradually decreases, from 0.39×10^5 N in the third rolling, to 0.09×10^5 N in the seventh rolling.

Considering the changes in the compaction degree and contact force chain, after five times of rolling, the compaction degree of the compacted soil and the thickness of the rolling layer change with the increase in rolling times, but the overall change amplitude is very small, and the contact force chain between the particles is also in a relatively stable state. If the rolling is continued on this basis, the saturation of the soil sample will likely increase due to excessive rolling, which will promote the development of the soil sample from dry to wet, and reduce its bearing strength. Therefore, the reasonable rolling amount obtained by discrete element simulation is five times.

4.3.2. Analysis of the Relationship between the Compaction Effect and the Rolling Process

Using the above discrete element model, the rolling simulation with a water content of 15% and rolling amount of five times was carried out. By changing the amplitude of the excitation force, the compaction effect of strong vibration and weak vibration rolling was analyzed. In the rolling process, the model is first subjected to static load rolling, and then strong vibration rolling and weak vibration rolling. When the weak vibration is applied, the amplitude of the excitation force is 1, and the magnitude of the excitation force is 928 N. When the strong vibration is applied, the amplitude of the excitation force is 2, and the magnitude of the excitation force is 1856 N.

It can be seen from Figure 12 that compared with the static rolling effect, both strong vibration and weak vibration rolling can greatly improve the compaction effect of subgrade rolling. The larger the amplitude of the roller vibration, the more obvious the improvement of the compaction effect. The main reason for this phenomenon is that the eccentric roller will produce an exciting force when it rotates, which will exert a short-term continuous pulse impact on the compacted soil, so that the effect between the soil particles changes from static friction to dynamic friction, the soil pores are reduced, and the particle skeleton is denser. After the fifth rolling, the compaction degree of strong vibration + weak vibration combination rolling is significantly higher than that of only strong vibration rolling or only weak vibration rolling, and it is found that the compaction effect of strong vibration first and then weak vibration is stronger than that of weak vibration first and then strong vibration. For the soil samples with a water content of 15%, the best rolling compaction process obtained by discrete element simulation is static compaction once + strong vibration twice + weak vibration twice.

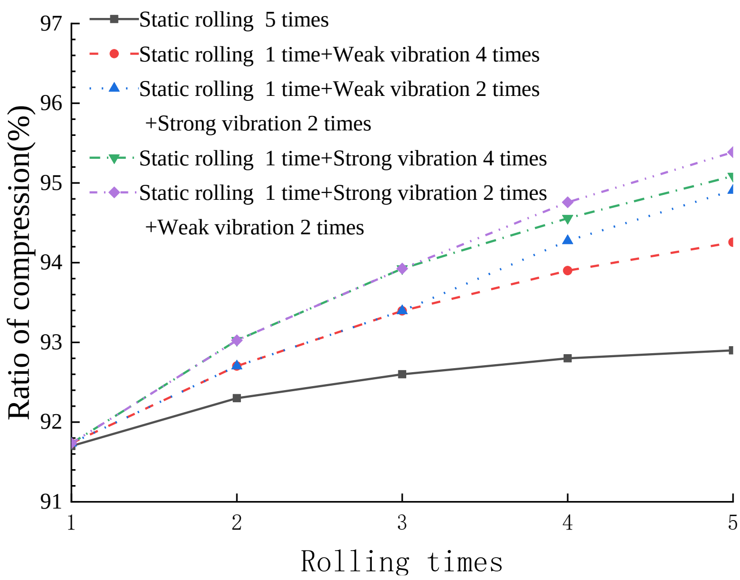

Figure 12. Relationship curve between the compaction times under static and dynamic loads and the compaction degree.

4.4. On-Site Compaction Process Analysis

The test area selected for the roadbed filling test is the second section of the main project of the reconstruction and expansion project from the Dezhou (Luji boundary) to the Qihe section of the Jingtai Expressway. The selected soil filler is a low liquid limit unsaturated silt in the soil field on the west side of the plain service area. At the engineering site, 3% cement was added to the unsaturated silt with a 15% water content, and its filler was modified. Then, the SEM8222 vibratory roller was used for strong vibration and weak vibration rolling, to determine the best compaction process. Table 5 is the changing table of the compaction degree under this condition.

Table 5. Variation of the compaction degree for different compaction combinations at 15% moisture content.

Compaction Combination	Degree of Compression
Static rolling 1 time + Weak vibration 2 times	90.8%
Static rolling 1 time + Weak vibration 3 times	92.2%
Static rolling 1 time + Weak vibration 4 times	94.6%
Static rolling 1 time + Weak vibration 5 times	95.3%
Static rolling 1 time + Strong vibration 3 times	93.2%
Static rolling 1 time + Strong vibration 4 times	96.4%
Static rolling 1 time + Strong vibration 5 times	94.3%
Static rolling 1 time + Weak vibration 2 times + Strong vibration 2 times	96.6%
Static rolling 1 time + Strong vibration 2 times + Weak vibration 2 times	98.1%

According to Table 5, it can be seen that improving the compaction effect of the soil samples by strong vibration or weak vibration alone is not obvious, and the compaction effect is better when only static rolling once + strong vibration four times. Compared with strong vibration rolling four times, the compaction degree decreases when the strong vibration rolling is carried out five times. The main reason for this phenomenon is that with the increase in the number of strong vibration rolling, the porosity of the soil sample gradually decreases, the water content increases, and the upper surface soil is bonded to the rolling wheel, which leads to the phenomenon of 'peeling' in the subgrade soil, leading to the decrease in the compaction degree.

The compaction effect of combined rolling is stronger than that of strengthening vibration and weak vibration alone. For combined rolling, both types of combinations can meet the compaction requirements of the first-class expressway, especially static rolling once + strong vibration twice + weak vibration twice, and the maximum compaction degree (98.1%) is reached when rolling five times. Considering the economic and environmental protection construction requirements, for an unsaturated silt with the best water content of 15%, the best compaction process is static pressure once + strong vibration twice + weak vibration twice, which is consistent with the discrete element simulation results.

5. Conclusions

In this paper, the discrete element software, PFC3D, is used to simulate and analyze the static triaxial test, and the rolling compaction process simulation and engineering field measurement are carried out to obtain the best rolling compaction process of soil samples under the best water content. The following conclusions are drawn:

(1) This article relates matrix suction to water content and uses matrix suction to approximate the water content state of soil samples. By comparing the results of the discrete element simulation triaxial compression test with the indoor triaxial compression test, the microscopic parameters of the unsaturated soil model were calibrated, and the accuracy of using matrix suction to characterize the water content state was verified. The feasibility of using Hill contact simulation of unsaturated soil was also confirmed.

(2) During the simulation of the rolling process using the PFC3D software, it was found that the relationship between the number of static rolling and the degree of compaction is proportional. The change in compaction degree in the whole rolling process can be divided into two stages: the first stage is the initial rolling stage, and the compaction degree of the model increases rapidly in this stage. The second stage is the re-grinding stage. The particles are relatively stable, and the increase in compaction degree is not significant. The reasonable rolling times are preliminarily determined to be five times, according to discrete element simulation.

(3) Through PFC3D software simulation, the changes in compaction degree under different rolling process combinations under the optimal moisture content conditions were analyzed. The results showed that compared with static compaction, both strong and weak vibration compaction can significantly improve the compaction effect of the roadbed compaction model. The larger the amplitude of the roller vibration, the

more obvious the improvement of this compaction effect. For the combination of strong vibration and weak vibration compaction, the compaction effect of strong vibration followed by weak vibration is stronger than that of weak vibration followed by strong vibration.

(4) Taking the unsaturated silt roadbed of the Dezhou-Qihe section of the Jingtai Expressway as the research object, the rolling test of a cement-modified unsaturated silt roadbed under the optimum moisture content was carried out using a field test to determine the optimum rolling compaction combination under this moisture content. According to the field test data, it can be seen that when the water content is 15%, the best compaction combination is static rolling once + strong vibration twice + weak vibration twice, which is consistent with the discrete element simulation results and has a certain guiding role in the construction of the project site.

Author Contributions: Conceptualization, Z.M.; Methodology, Z.M. and K.L.; Software, K.L. and D.S.; Validation, D.S.; Formal analysis, W.L., Y.W. and S.L.; Investigation, W.L.; Data curation, Y.W. and S.L.; Writing—original draft, K.L.; Writing—review & editing, K.L.; Visualization, D.S.; Supervision, Z.M.; Project administration, Z.M.; Funding acquisition, Z.M. All authors have read and agreed to the published version of the manuscript.

Funding: This research received no external funding.

Institutional Review Board Statement: Not applicable.

Informed Consent Statement: Not applicable.

Data Availability Statement: Data available on request from the authors.

Conflicts of Interest: The authors declare no conflict of interest.

References

1. Ma, H.J. Elementary discussion on disposal method of subgrade filling over-wet soil. *Urban Roads Bridg. Flood Control* **2014**, *184*, 35–36. [CrossRef]
2. Xu, X. The strength and deformation characteristics of unsaturated soil at high suction and low stress. Doctor's Thesis, Beijing Jiaotong University, Beijing, China, 2019.
3. Shi, J.G.; Shao, S.J.; Tao, H.; Xu, P. True triaxial tests and strength deformation behaviors of unsaturated soils. *Chin. J. Geotech. Eng.* **2011**, *33*, 92–97.
4. Ye, L.M. Study on Engineering Characteristics of Unsaturated Silt Subgrade in Drying and Wetting Cycle. Master's Thesis, Zhengzhou University, Zhengzhou, China, 2014.
5. Chen, Z.H.; Guo, N. New developments of mechanics and application for unsaturated soils and special soils. *Rock. Soil. Mech.* **2019**, *40*, 1–54. [CrossRef]
6. Guo, Y.; Chi, S.C.; Mi, X.F. Experimental study on particle strength and elastic mechanical parameters of coarse-grained soil. *Chin. J. Geotech. Eng.* **2021**, *43*, 1675–1681. [CrossRef]
7. Kuhn, M.R.; Suzuki, K.; Daouadji, A. Linear-frictional contact model for 3D discrete element simulations of granular systems. *Int. J. Numer. Meth. Eng.* **2020**, *121*, 560–569. [CrossRef]
8. Kuhn, M.R.; Daouadji, A. Simulation of undrained quasi-saturated soil with pore pressure measurements using a discrete element (DEM) algorithm. *Soils Found.* **2020**, *60*, 1097–1111. [CrossRef]
9. Liu, S.H.; Sun, D.A.; Wang, Y. Numerical study of soil collapse behavior by discrete element modelling. *Comput. Geotech.* **2003**, *30*, 399–408. [CrossRef]
10. Liu, S.P. Three Dimensional Liquid Bridge Contact Model and Discrete Element Numerical Simulation Study of Unsaturated Soil. Master's Thesis, Beijing Jiaotong University, Beijing, China, 2019. [CrossRef]
11. Zhou, F.X.; Zhao, M.; Ying, S. Analysis of mechanical behavior for unsaturated soil by three-dimensional discrete element method. *J. Fuzhou Univ. (Nat. Sci. Ed.)* **2020**, *48*, 779–785.
12. Zhang, N. Three-Dimensional Numerical Analysis of the Compaction Properties of RCC Based on DEM. Master's Thesis, Zhejiang University, Hangzhou, China, 2015.
13. Yan, X.; Feng, Z.C.; Huang, G.Q. Research on construction technology of low liquid limit powder roadbed for highway. *Highway Transp. Technol. (Appl. Technol. Ed.)* **2019**, *15*, 47–49.
14. Cai, L. Analysis of construction technology of low liquid limit powder roadbed. *Highway Transp. Technol. (Appl. Technol. Ed.)* **2020**, *16*, 63–65.
15. Potyondy, D. *Material-Modeling Support in PFC [fistPkg25]*; Technical Memo; Itasca Consulting Group: Minneapolis, MN, USA, 2017; ICG7766-L.

16. Cundall, P.A. Computer simulations of dense sphere assemblies. *Stud. Appl. Mech.* **1988**, *20*, 113–123. [CrossRef]
17. Potyondy, D.O. The Bonded-Particle Model as a Tool for Rock Mechanics Research and Application: Current Trends and Future Directions. *Geosyst. Eng.* **2015**, *18*, 1–28. [CrossRef]
18. Xu, K.; Huang, W.X.; Huang, L.Y. Numerical simulation and analysis of roller compaction of granular soil. *Yellow River* **2014**, *36*, 124–127.